

# Deconvolution of immittance data: Some old and new methods

J. Ross Macdonald <sup>a,\*</sup>, Enis Tuncer <sup>b</sup>

<sup>a</sup> *Department of Physics and Astronomy, University of North Carolina, Chapel Hill, NC 27599-3255, USA*

<sup>b</sup> *Applied Superconductivity Group, Fusion Energy Division, Oak Ridge National Laboratory, Oak Ridge, TN 37831-6122, USA*

Received 26 September 2006; received in revised form 29 December 2006; accepted 11 January 2007

Available online 14 January 2007

## Abstract

The background and history of various deconvolution approaches are briefly summarized; different methods are compared; and available computational resources are described. These underutilized data analysis methods are valuable in both electrochemistry and immittance spectroscopy areas, and freely available computer programs are cited that provide an automatic test of the appropriateness of Kronig–Kramers transforms, a powerful non-linear-least-squares inversion method, and a new Monte Carlo inversion method. The important distinction, usually ignored, between discrete-point distributions and continuous ones is emphasized, and both recent parametric and non-parametric deconvolution/inversion procedures for frequency-response data are discussed and compared. Information missing in a recent parametric measurement-model deconvolution approach is pointed out and remedied, and its priority evaluated. Comparisons are presented between the standard parametric least squares inversion method and a new non-parametric Monte Carlo one that allows complicated composite distributions of relaxation times (DRT) to be accurately estimated without the uncertainty present with regularization methods. Also, detailed Monte Carlo DRT estimates for the supercooled liquid  $0.4\text{Ca}(\text{NO}_3)_2 \cdot 0.6\text{KNO}_3$  (CKN) at 350 K are compared with appropriate frequency-response-model fit results. These composite models were derived from stretched-exponential Kohlrausch temporal response with the inclusion of either of two different series electrode-polarization functions.

© 2007 Elsevier B.V. All rights reserved.

**Keywords:** Deconvolution; Inversion; Distributions of relaxation times and activation energies; Least-squares methods; Regularization; Monte Carlo inversion; Electrode effects

## 1. Background

Both electrocatalysis and immittance spectroscopy data usually involve distributions of relaxation times or activation energies, but because methods of estimating such distributions, called deconvolution or inversion, are thought to be difficult to apply or not readily available, such techniques for aiding in understanding physico-chemical processes present in materials are often underutilized. A list of acronym definitions, including ones for fitting models, is included at the end of the present work.

Deconvolution is a procedure for transforming data, usually in temporal- or frequency-domain form, to the relaxation-time,  $\tau$ , realm. It allows one to re-express the data in terms of an overall distribution of relaxation times (DRT). Such a DRT may represent a single relaxation/dispersion physical process or may show individual DRT regions representing several such processes. In the latter case, mean relaxation times for some or all of the processes may be identified, depending on their degree of overlap, directly from a plot of the results. In addition, DRT analysis also provides estimates of specific Debye-type relaxation times and individual strength parameters. Such analysis can also lead to the estimation of distributions of activation or adsorption energies often present in solid or liquid materials and especially in electrochemistry. Further, DRT analysis may be used to check the applicability of the

\* Corresponding author. Tel.: +1 919 967 5005; fax: +1 919 962 0480.  
E-mail addresses: [macd@email.unc.edu](mailto:macd@email.unc.edu) (J.R. Macdonald), [tuncere@ornl.gov](mailto:tuncere@ornl.gov) (E. Tuncer).

Kronig–Kramers integral–transform equations for limited-range data and to estimate the real or imaginary part of the data when only the other part is available.

The DRT-estimation approach is superior to the model-based one involving an explicit data-fitting expression because DRT estimation requires no *a priori* assumptions, but it is inferior in that it leads to less detailed information about the processes present. In many situations it is thus useful first to deconvolve the data and then use the results to help decide on an appropriate fitting model and to estimate initial values of some of the parameters of such a specific fitting model. Fitting the data with such a model can then yield more detailed information about the physical situation, especially when it involves one or more distributed elements such as the constant-phase one [1].

Many approaches to DRT estimation, going back at least to the 1907 work of von Schweidler and its 1913 generalization by Wagner [2], are summarized in Ref. [3]. Summaries of relevant work from 1970 to 1995 appear in the dielectric-data inversion work of [4]; in the 1988 work of Kliem et al. [5]; and in a 1999 electrochemically oriented chapter [6]. Until recently, there were two main techniques used to estimate DRTs: regularization methods [6–8] and parametric linear or non-linear least squares fitting (PLS) [4,8,9]. The regularization approach has been evaluated in detail in [6] and has been compared with the PLS one in Ref. [8], where the latter was found to be appreciably superior for the situations considered. The only readily available free version of a computer program that includes algorithms for both regularization and PLS is a part of the LEVM complex-non-linear-least-squares (CNLS) program described in Refs. [8,10]. A newly developed third method is based on Bayesian statistics and involves a Monte Carlo technique [11,12].

In the rest of the present work, recent DRT analysis methods are considered, compared to earlier ones, put in historical perspective, and their usefulness evaluated.

## 2. Least-squares deconvolution methods

The regularization method, essentially a non-parametric approach, involves a regularization parameter whose value is chosen to ameliorate inversion problems by a kind of smoothing process, one that necessarily introduces some inaccuracy in DRT estimation. Here emphasis is on the PLS approach for estimating an unknown DRT,  $g(\tau)$  or a transformation of it [13]. It involves expressing the frequency-response data,  $I(\omega)$ , as an integral from zero to infinity over  $g(\tau)/[1 + i\omega\tau]$ , or temporal data,  $f(t)$ , as an integral over  $g(\tau)\exp(-t/\tau)$  [3,4,13]. These integrals must then be inverted to obtain estimates of  $g(\tau)$ . For the usual case of numeric data [4,8–10,13], the integrals are approximated by finite sums of the forms

$$I(\omega) = \sum_{m=1}^M g_m/[1 + i\omega\tau_m], \quad (1)$$

and

$$f(t) = \sum_{m=1}^M g_m \exp(-t/\tau_m), \quad (2)$$

where  $g_m$  is a strength parameter,  $\tau_m$  the characteristic Debye relaxation time, and  $g_m$ 's are often normalized by transforming them to  $G_m \equiv g_m/\sum_{m=1}^M g_m$ , leading to  $I(0) = 1$ .

It is often useful to write deconvolution equations in terms of logarithmic variables. If one defines  $y \equiv \ln(\tau/\tau_0)$ , then we may write in terms of continuous variables (13),

$$I(\omega) = \int_{-\infty}^{\infty} F(y) dy/[1 + i\omega\tau_0 \exp(y)], \quad (3)$$

where  $\tau_0$  is an arbitrary, fixed relaxation time, and  $F(y) \equiv \tau g(\tau)$ . When raw data are used in deconvolution, both sides of Eq. (3) should be multiplied by  $\Delta U$ , where  $\Delta U \equiv U(0) - U(\infty)$ , and  $U(\omega) = \rho(\omega)$  or  $\varepsilon(\omega)$  for conductive or dielectric DRT situations, respectively. It follows from Eq. (3) that when  $F(y)$  is normalized, the usual case, then  $I(0) = 1$ , while when it is not,  $\Delta UI(0) = \rho(0) - \rho(\infty) \equiv \rho_0 - \rho_\infty$  for a conductive system, one where  $\rho_\infty$  is usually zero or negligible.

For dipolar dielectric frequency response, assumed to involve dispersion associated with a distribution of dielectric relaxation times, we shall denote the distribution as  $F_D(y)$ , and  $I(\omega)$  will then represent the associated dielectric-level normalized frequency response. For conductive-system dispersion associated with mobile ions, assumed to be representable by a distribution of resistivity relaxation times, we use  $F_C(y)$ , and  $I(\omega)$  is the normalized complex resistivity level frequency response when  $F_C(y)$  is normalized. When the distribution involves data involving more than a single relaxation process, a composite frequency-response fitting model, such as one that accounts for electrode polarization effects as well as bulk dispersion, is usually most appropriate and its associated composite distribution will be denoted as  $\Delta UF(y)$ .

In practice, PLS deconvolution generally starts with the choice of a small value of  $M$ , the number of elemental Debye responses in the fit of Eq. (1) or (2), and for succeeding fits  $M$  is sequentially increased to a maximum value,  $M_{\max}$ , with halting when a good fit is achieved.  $M_{\max}$  should always be appreciably smaller than the number of data points.

The rest of the present work deals with the important case of DRT estimation using frequency-response data. Note that when the  $I(\omega)$  of Eq. (1) involves impedance or complex resistivity data, one deals with a sum of Voigt response elements (each one equivalent to a resistor and capacitor in parallel) and the DRT estimated from such data is a distribution of impedance relaxation times, while when complex dielectric data is deconvolved, one obtains a distribution of dielectric relaxation times involving Maxwell elements (represented by a resistor and capacitor in series) [4].

When a least squares fit is used to estimate values of  $g_m$  with the  $\tau_m$  parameter values fixed, usually uniformly on a logarithmic scale, the estimation problem is linear and readily carried out. Define it as PLLS. In contrast, when both types of parameters are free to vary, the most accurate approach [4,8], the situation is non-linear and CNLS must be used for full complex data. This inversion process is usually appreciably more difficult and is here designated by PNLS. Both PLLS and PNLS fitting of real-part, imaginary-part, or full complex data usually involve data weighting, and many choices are included in the LEVM deconvolution algorithms [10]. Although the authors of a recent PLS DRT analysis approach mention that their inversion program was written “in house,” it is neither fully described nor stated to be available for use by others [14]. Further, their approach is characterized as involving non-linear regression but it seems to involve only PLLS rather than PNLS, as discussed below.

### 3. Recent DRT analyses and comparisons

#### 3.1. PLS inversion approaches

The 2002 PLS publication of Ref. [14] stated that methods of obtaining information about DRTs were not well developed and proposed “a method for identification, from impedance spectra, of the distribution of time constants associated with activation or relaxation processes.” Their approach, although not so mentioned, is just a version of the PLS one described much earlier by others and instantiated in the PLLS and PNLS approaches included in the widely used LEVM program and its predecessor, the LOMFP program of 1988. Further, Ref. [14] work is a follow-on of the 1992–1995 work of Agarwal et al. [15], where the deconvolution approach described in their 1992 publication was named the “measurement model” and originally used the LOMPF fitting program. It is pointed out in Ref. [15] that a good-fit value of  $M_{\max}$  leads to estimates of fitting residuals (termed stochastic error structure there) and thus may be helpful in choosing appropriate weighting for subsequent fits of the data.

Recently, Farag et al. [16], in a follow-up of the work of Ref. [5], also tackled the problem of data inversion using an iterative numerical technique different from and less accurate than the CNLS procedure used in LEVM [10]. Their method starts with the assumption of a box-like DRT, requires smoothing, and iterates toward a final approximate distribution.

It is worth noting that the two main features of a PLS (or measurement model) approach: that fitting data to a physically realizable, practical model such as that of Eq. (1) would automatically ensure satisfaction of the Kronig–Kramers (KK) integral–transform relations, and implying that any such model could be used for this purpose, appeared in Ref. [17] in 1987. Although these ideas were thus current several years before the independent introduction of the term “measurement model” and its

use of a specific circuit model of Voigt elements, as in the 1988 LOMPF fitting program, no such provenance was mentioned in Refs. [14] and [15].

It is also noteworthy that in both Refs. [7,14] it is stated that DRT estimation from experimental data is a mathematically ill-posed problem, leading to great sensitivity to experimental errors. But these authors made no distinction between discrete and continuous DRTs and perhaps implicitly assumed that the data involved only continuous ones. In Ref. [4] it was shown, however, that there is a crucial difference between the inversion of data involving a continuous distribution of relaxation times and one involving a discrete distribution. Although in the numerical analysis both situations are approximated by a discrete set of Debye relaxations, these two types of response can be distinguished [4,18–20], and it turns out that inversion of data associated with a discrete set of time constants is not ill-posed, in contrast to the continuous DRT situation. Extensive PNLS DRT estimation and Kronig–Kramers analysis carried out in Refs. [4,18–20] also considered analysis and identification methods for situations involving not only a continuous DRT but also some discrete relaxation points. In addition, the method used in Ref. [11] utilizes a Monte Carlo Technique and overcomes the ill-posed character of data inversion by estimating the distribution of the relaxation times in each Monte Carlo step. This novel implementation of the Monte Carlo method makes the relaxation time axis essentially continuous and less sensitive to initial-guess parameter values, unlike previous techniques.

In 1995 Boukamp showed, in contrast to ordinary PNLS inversion, where both strength and relaxation-time parameters are free to vary and all parameter estimates are required to be positive for most data situations, that when the  $\tau_m$  relaxation parameter values were taken fixed and the free strength parameters values were not restricted to be positive, the resulting PLLS inversion procedure became linear and simpler and its results, although not usually physically plausible, could nevertheless be used to test for satisfaction of the KK relations [21]. Such choices have also been an implicit part of the LEVM fitting and inversion program since its inception, and in 2004 Boukamp made freely available his KKTEST PLLS program, one that automatically evaluates data for KK appropriateness. It involves about seven fixed  $\tau_m$  values per decade and so can well evaluate the quality of wide-range data.

Orazem and his co-authors state, in their 2002 Ref. [14] work, that an important objective was to study the effect on deconvolution results of adding 1% stochastic noise to the impedance data they considered. Unfortunately, they were evidently unaware that the effects of both 1% and 4% noise was studied much more comprehensively in 2000 [8,9]. In addition, they examined the effects on DRT estimation of truncating their data at low frequencies with or without 1% errors. Again, they did not refer to an earlier detailed study of such truncation effects [9], where no errors, 1% ones, and 4% ones were added and the resulting relative

fitting errors present in the estimated DRT results were presented for some of the inversions. In 2001 Tuncer and Gubanski [11] also investigated the influence of 5% measurement errors on their Monte Carlo method and showed that unique distributions could be recovered even if the data contained large errors.

### 3.2. Discussion and illustration of the utility of several different deconvolution methods

#### 3.2.1. Comparison of two inversion methods for a dielectric situation

A limitation of the usual PLS inversion procedure instantiated in LEVM [10] is that the maximum value of the  $M$  in Eqs. (1) and (2) is currently restricted to 19. The results cited in Ref. [14] involve even smaller values. Although  $M = 19$  or less is quite sufficient for DRTs representing a single physical process, it may limit the resolution of inversion results for multiple-process data, such as the simultaneous presence of bulk dispersion response and that associated with electrode polarization and adsorption processes. It is therefore fortunate that an alternate non-parametric deconvolution approach has been recently developed [11], one that does not involve an upper limit to  $M$  and also avoids the uncertainties associated with the choice of the regularization parameter in deconvolution using regularization, even though this method can also deal approximately with multiple-process data.

The 2001 work of Tuncer and Gubanski [11] provided an alternative to allowing relaxation times to be free variables for ill-posed continuous-distribution inversion situations. In this essentially non-parametric method, a Monte Carlo procedure based on constrained least squares is used to closely approximate the time or frequency axis as continuous. In this method, Eq. (1) is solved with fixed relaxation-time values, randomly selected from a log-linear range. This procedure converts the non-linear problem to a linear one with only the  $g_m$  parameters as unknowns. The set of fixed relaxation times is varied in each Monte Carlo step. Finally, the weighted distribution of  $g_m$  vs.  $\tau_m$  yields  $\Delta U F(y)$ .

For the present data deconvolutions, 66 pre-assigned  $\tau$  values were used with  $2^{15}$  Monte Carlo steps, resulting in 2,162,688 final  $\tau_m$  values, close to continuous. A recent comparison between the inversion of continuous distributions by the PNLLS approach (Method I) and that of Ref. [11] (Method II) shows the strengths and weaknesses of both methods [22]. One of its main results is replicated in Fig. 1.

In the present work, we shall be primarily concerned with two different but closely related frequency-response bulk models, both involving a shape parameter  $\beta$  that satisfies  $0 < \beta \leq 1$ . These two models, discussed in detail in Ref. [23], are the conductive-system K1 one, where we set  $F_C = F_1$  and  $\beta = \beta_1$ , and the dielectric-system KD one, involving the  $F_D$  DRT and a  $\beta_D$  shape parameter. Both models also involve a dc resistivity,  $\rho_{C0}$  or  $\rho_{D0}$ , and a char-

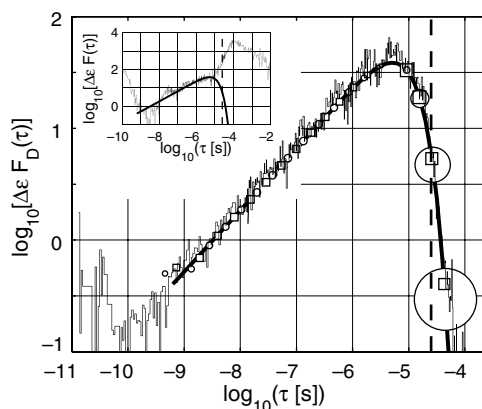


Fig. 1. Unnormalized distributions of relaxation times derived from synthetic frequency-response data using methods I and II [22], compared to the known unnormalized KD distribution, shown as a thick solid line. Method-I DRT results are shown for inversion using only the real part of the data (open square symbols) and for only the imaginary part (open circle symbols). The symbol sizes are proportional to the individual estimated uncertainties of the fit points. The method-II results, shown as solid stair lines, used the full complex data. The vertical dashed line shows the position of the characteristic relaxation time of the KD model, 2.63  $\mu$ s. The inset compares the known bulk-model distribution to that derived from the raw experimental data using method II.

acteristic time constant  $\tau_{C0}$  or  $\tau_{D0}$ . The KD model is a one-sided Fourier transform of stretched-exponential temporal response and the K1 is derived from such response but involves a different DRT [23]. In this section, we deal with a dielectric-response system and in the next with a conductive-system one.

In its inset, Fig. 1 shows method-II deconvolution results using full experimental frequency-response complex data [22], expressed at the dielectric level. Although this experimental data set actually involved dispersion arising from mobile ions best described by a K1 model, parameters estimated from fitting it with a composite KD model that also included a series electrode-polarization function [4,10,23,24] were used to generate complex dielectric-level KD-model synthetic data over a wide frequency range. The fit led to a  $\beta_D$  estimate of about 0.55. The resulting nearly exact synthetic data set was then deconvolved to estimate the DRT of the dispersed response, taken to be of dielectric character. Method I and II inversion results are compared to the exact  $F_D$  KD-model DRT in the main part of Fig. 1. It is worth noting the little-known fact that the K1 and KD DRTs are of exactly the same form when  $\beta_1 = \beta_D$  [23].

Since the true DRT may be accurately calculated directly for a known KD frequency-response model [10], the resulting  $F_D$  response is used here as a standard with which to compare the results of applying methods I and II. Experimental data at the complex dielectric constant level may be represented by  $\varepsilon(\omega) - \varepsilon(\infty) = \Delta\varepsilon I(\omega)$ , where  $\Delta\varepsilon \equiv \varepsilon(0) - \varepsilon(\infty)$ , and  $I(\omega)$  is defined in Eq. (3). Direct deconvolution of such data then leads to the unnormalized  $\Delta\varepsilon F$  and  $\Delta\varepsilon F_D$  DRT estimates shown in the figure.

The results in Fig. 1 demonstrate that both methods quite accurately estimate the true DRT in the absence of systematic and random noise in frequency-response data. It is clear that the method-I real-part inversion leads to much more accurate DRT estimates in the region to the right of the peak than does the imaginary-part inversion. Both method-I estimates are more accurate than is the method-II one for  $\tau$  values less than the peak one. But note that method-II yields an approximate extrapolation of the DRT by as much as a decade beyond the low- $\tau$  limit of the method-I DRT estimates. The method-II inset of Fig. 1 shows inversion results using the full experimental data, again compared to the true bulk DRT. It is evident that an added distribution appears with a peak near 100  $\mu$ s, well beyond the bulk DRT response. This distribution is clearly associated with partially blocking electrode-polarization effects, in agreement with the composite-model frequency-response fitting of the data.

### 3.2.2. The differential impedance analysis (DIA) method

This approach involves a deterministic model with numerical differentiation of the real and imaginary parts of impedance data [7,25]. Since such differentiation can itself lead to ill-posed results for noisy data, the DIA procedure involves the use of spline-fitting for smoothing when appropriate. It seems to be most appropriate for analyzing data involving discrete distributions of relaxation times and involves a “spectral transform,” one that shows spectral peaks.

Most experimental data response is best analyzed by assuming that it arises from the presence of one or more distributed circuit elements, ones that involve a continuous DRT, as discussed and illustrated in Section 3.2.1. DIA analysis has apparently not been used to estimate a continuous DRT from exact or noisy synthetic data and to compare it with the exact DRT that led to the data. In spite of uncertainties associated with numerical differentiation and with how much smoothing to use, the method has been shown to lead to useful DRT estimates for various synthetic and experimental data sets [25], but it is not clear how well it could be adapted to take proper account of the presence of parallel and series additions to a main bulk response model involving a continuous DRT. The importance of such distorting effects and their removal are illustrated for a composite-response model in Section 3.2.3.2.

### 3.2.3. Frequency-response fitting and inversion of limited data

Here we consider both frequency-response fitting and inversion of limited-range data for the supercooled liquid  $0.4\text{Ca}(\text{NO}_3)_2 \cdot 0.6\text{KNO}_3$  (CKN) at 350 K. Although it is conventional to consider that the response of this material is dominated by ionic conduction, we shall also demonstrate how well the data can be fitted by assuming dielectric rather than resistivity dispersion. In both cases, it was found that good fits were only possible using a composite model that included bulk-dispersion response associated

with either K1 or KD and a series model S. All frequency-response fitting models used herein are defined in the list of acronyms at the end of this work.

**3.2.3.1. Frequency-response data fitting.** Fig. 2 shows results of conductive-system CK1S fits of the frequency-response data. The symbol C denotes a specific capacitance that models the bulk high-frequency-limiting dipolar dielectric constant  $\varepsilon_{D\infty}$ . It is in parallel with the K1 model, and the result is in series with a response model S, usually representing electrode polarization. Two different functions were used here for S: a series constant-phase element, SCPE, expressed at the conductivity level as  $\sigma_{SC} \equiv \varepsilon_V A_{SC} (i\omega)^{\gamma_{SC}}$ , and a series Cole–Davidson (CD) model, expressed at the resistivity level as  $\rho_{CD} \equiv \rho_{0S} / [1 + (i\omega\tau_{0S})]^{\gamma_S}$ . The S parameters are all frequency independent, and  $\varepsilon_V$  is the permittivity of vacuum.

Table 1 fitting results show that although the row-4 CK1CD-model fit is the best, it is not substantially better than those of the other two composite models. Note that the K1 model involves an additional high-frequency-limiting dielectric constant,  $\varepsilon_{C1\infty}$ , arising entirely from charge motion and readily calculated from K1-model fit results [23]. It follows that for such fits the full frequency-limiting dielectric constant is  $\varepsilon_{\infty} = \varepsilon_{C1\infty} + \varepsilon_{D\infty}$ . When no free parameter representing  $\varepsilon_{D\infty}$  is included in a K1 fit, so the bulk fit model is that of K1 rather than CK1, the resulting

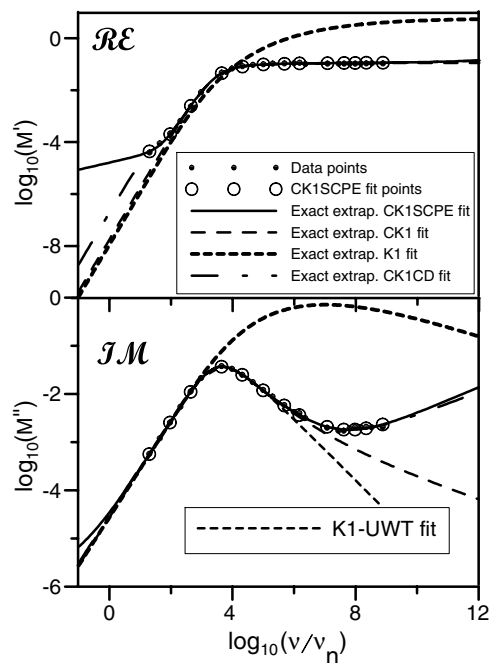


Fig. 2. Data and various modulus-level frequency-response fit results for the KCN material at 350 K. Most of the extrapolated lines extending beyond the data at both low and high frequencies were calculated using parameter estimates following from fitting using the CK1SCPE composite model discussed in the text, but some are also shown for CK1CD-model fitting. The K1 fit using unity weighting is an example of the erroneous original modulus formalism approach. Parameter estimates are listed in Table 1. Here  $v_n$  is 1 Hz.

Table 1  
Parameter estimates for 350-K CKN frequency-response data. The composite fitting models involved K1 and KD bulk models with added SCPE or CD series electrode polarization functions

#	Model	100 $S_F$	$\rho_{C0}$ ( $\Omega$ cm)	$\tau_{C0}$ [ $\tau_{D0}$ ] (s)	$\beta_1$ [ $\beta_D$ ]	$\varepsilon_{C1\infty}$ [ $\Delta\varepsilon$ ]	$\varepsilon_{D\infty}$ [ $\varepsilon_\infty$ ]	$10^{-6}\rho_{0S}$ ( $\Omega$ cm)	$A_{SC}$ [ $10^3\tau_{0S}$ ] (s)	$\gamma_{SC}$ [ $\gamma_S$ ]
<i>S = SCPE</i>										
1	CK1SCPE	5.8	$4.92 \times 10^7$	$9.7 \times 10^{-9}$	0.212	0.169	8.82	–	$9.26 \times 10^4$	0.728
2	K1-DRT (unnorm.)	–	$1.73 \times 10^{12}$	$5.1 \times 10^{-8}$	0.209	–	–	–	–	–
3	K1-UWT $M''$ fit	–	$4.92 \times 10^7$ (fixed)	$2.90 \times 10^{-5}$	0.643	–	[9.20]	–	–	–
<i>S = CD</i>										
4	CK1CD	5.1	$4.82 \times 10^7$	$2.6 \times 10^{-8}$	0.232	0.230	8.78	7.06	[9.58]	[0.754]
5	K1-DRT (unnorm.)	–	$1.26 \times 10^{12}$	$1.4 \times 10^{-7}$	0.229	–	–	–	–	–
6	K1-UWT $M''$ fit	–	$4.82 \times 10^7$ (fixed)	$2.87 \times 10^{-5}$	0.647	–	[9.25]	–	–	–
7	CKDCD	5.4	4.83	[ $3.0 \times 10^{-4}$ ]	[0.414]	[13.5]	[9.26]	7.25	[9.69]	[0.745]

Complex non-linear least squares fits were carried out using proportional weighting for all but rows 3 and 6, where unity weighting of the  $M''(\omega)$  data was employed.  $S_F$ , the relative standard deviation of the fit residuals, is a measure of the goodness of fit. Data were fitted at the complex resistivity level for the CK1SCPE and CK1CD fits and at the complex dielectric level for the CKDCD one. The K1-DRT results are for the unnormalized conductive-system DRTs estimated using the Monte Carlo inversion method. Square brackets are used to allow easy discrimination between situations.

still widely used but erroneous 1973 original modulus formalism approach of Moynihan et al. [26] leads to a  $\varepsilon_{C1\infty}$  estimate of  $\varepsilon_\infty$ , as shown in rows three and six of the table, thus inconsistent with a purely conductive-system model [13,23,27]. Note the vast high-frequency differences shown in Fig. 2 between the K1 and CK1 responses, both calculated from the appropriate CK1SCPE-fit parameter estimates.

Although Fig. 2 shows only a very small difference between the  $M''$  responses of the CK1SCPE and CK1CD models at high frequencies, there is a large difference in their low-frequency  $M'$  responses, even though both led to equally good fits of the data in this region. Had the data extended to lower frequencies by even a relatively small amount, discrimination between the two series response models would have been greatly improved.

Particularly interesting are the high-frequency  $M''$  differences between the data, well represented by the full composite-model fits, the CK1 and K1 responses calculated from the full CK1SCPE fit, and the K1-UWT fit line. Clearly, the CK1 part of the response is inadequate here without a series-response contribution and shows an excess wing, but the excess is far greater for the direct fit of the K1 model alone using unity weighting instead of proportional weighting; also see row-3 in the table. Such UWT fitting, carried out for  $M''$  data extending only to  $10^5$  Hz, emphasizes the largest  $M''$  values and is closely equivalent to results that would be obtained using the Moynihan original modulus formalism [26].

Note that the CK1 fit line deviates at higher frequencies from its lower-frequency straight line above the peak of the  $M''$  response. Such response is characteristic of situations where the ratio  $\varepsilon_{D\infty}/\varepsilon_{C1\infty}$  is very large, as it is here, and K1 response then only dominates at the higher frequencies [23], adding to the difficulty of accurate data analysis.

3.2.3.2. Monte Carlo estimation results. Fig. 3 shows the results of a Monte Carlo inversion of the original data as well as inversions of synthetic data. For these unnormal-

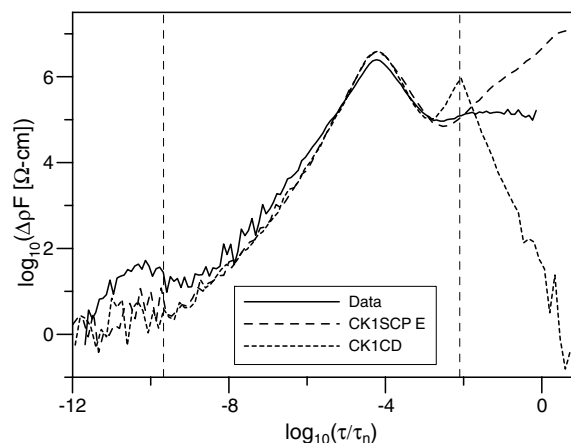


Fig. 3. Unnormalized  $\Delta\rho F$  DRT inversion results for the original 350 K CKN data and wide-range synthetic data calculated from conductive-system fits of the original data for two different series response functions. Here and elsewhere  $\tau_n = 1$  s.

ized results the  $\Delta\rho$  values are those of  $\rho_{C0}$  in Table 1. The vertical dotted lines are the limits of the original frequency data converted to the  $\tau$  domain. The two inversions of synthetic data used data calculated from the estimated parameters of the Table 1 CK1SCPE and CK1CD fits of the original data with 261 points extending from 0.1 Hz to  $10^{12}$  Hz. Their  $\tau$  range is thus about  $1.59 \times 10^{-13} \leq \tau \leq 1.59$  s. We see that when the DRT strength parameters are less than about  $10^{-5}$  of their peak values, the results become more and more noisy.

Most interesting are the differences apparent for  $\tau > 10^{-3}$  s. Clearly, neither the SCPE nor the CD model well represents the response associated with the original data at this end of the range. But the DRT response estimated from the original data in the range beyond the vertical cut-off line is itself likely to be very uncertain. One can only suggest that a series response model different from either of the present ones might be more appropriate, and that only analysis of new data extending a decade or two higher in frequency could likely resolve the matter.

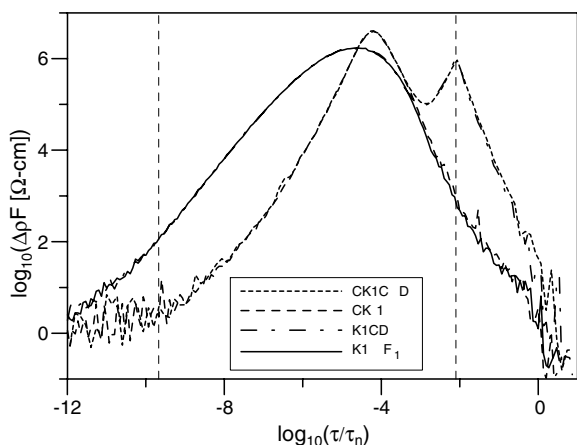


Fig. 4. Comparison of DRT responses for wide-range synthetic data derived from the CK1SCPE-model fit of the original data with deconvolutions involving data generated using fewer parameter estimates of that fit.

Fig. 4 shows deconvolution results only for synthetic data. The dissected CK1, K1CD, and K1 DRT curves were all calculated using frequency responses derived from the full-fit CK1CD estimated parameters. Note that the unnormalized K1 response designated K1  $F_1$  in the figure is that denoted  $\Delta\rho F_1$  in Section 2. The K1-DRT results of rows 2 and 5 of Table 1 show parameter estimates obtained by fitting the upper parts of the K1 inversion curves with the nearly exact K1 DRT model [10]. Although the  $\beta_1$  estimates are close to the original frequency-response fit ones, the DRT-fit  $\tau_{C0}$  estimates are appreciably different. This is because for the present small values of  $\beta_1$  there is a high correlation between  $\beta_1$  and  $\tau_{C0}$  estimates, and the uncertainties of the latter become very large for the frequency-response fits.

The narrowness of the CK1CD peak region compared to that for the K1 alone arises because the response of the former is dominated at  $\tau$  values below about  $\tau_T \equiv 10^{-3}$  s by nearly Debye response associated with the parallel combination of  $\rho_{C0}$  and  $\varepsilon_{D\infty}$ . It is consistent that the CK1 line follows the CK1CD response for  $\tau < \tau_T$  and the K1 line for  $\tau > \tau_T$ , while the K1CD line changes from K1 to CK1CD response near  $\tau_T$ . Finally, comparison of Fig. 2 results with those of Fig. 4 suggest that the full widths of comparable peaked frequency-response and DRT curves at half-height are closely related. It is clear that the present DRT inversion estimates usefully complement those obtained directly from PNLLS fits of experimental frequency-response data.

#### 4. Acronym definitions

##### General

CNLS	complex non-linear least squares
DIA	differential impedance analysis [7,25]
DRT	distribution of relaxation times
KK	Kronig–Kramers transform relations
LEVM	CNLS fitting and inversion program [10]
PLS	parametric least squares

PLLS	parametric linear least squares
PNLLS	parametric non-linear least squares
PWT	proportional weighting [10]
UWT	unity weighting [10]

##### Single and composite frequency-response fitting models

CD	Cole–Davidson response function defined at the impedance level (see Section 3.2.3.1)
K1	conductive-system Kohlrausch frequency-response model (see Section 3.2.1)
KD	dielectric-system Kohlrausch frequency-response model (see Section 3.2.1)
CK1	K1 model in parallel with a capacitance, C
CK1CD	CK1 model in series with a CD one
CK1S	CK1 model in series with a electrode-polarization model, S
CK1SCPE	CK1S model with S defined as a constant-phase-angle element
SCPE	series constant-phase element (see Section 3.2.3.1)

#### Acknowledgements

We thank Dr. P. Lunkenheimer for providing the present CKN data and he and Dr. B.A. Boukamp for valuable comments and suggestions. The work of Dr. E. Tuncer was sponsored by the US Department of Energy, Office of Electricity Delivery and Energy Reliability, Superconductivity Program for Electric Power Systems, under Contract No. DE-AC05-00OR22725 with Oak Ridge National Laboratory, managed and operated by UT-Battelle, LLC.

#### References

- [1] E. Barsoukov, J.R. Macdonald (Eds.), second ed., Impedance Spectroscopy: Theory, Experiment, and Applications, Wiley, New York, 2005.
- [2] E. von Schweidler, Ann. Phys. 4–24 (1907) 711; K.W. Wagner, Ann. Phys. 4–40 (1913) 817.
- [3] C.J.F. Böttcher, P. Boredewijk, Theory of Electric Polarization, third ed., Elsevier, New York, 1996, pp. 45–137 (Chapter 9).
- [4] J.R. Macdonald, J. Chem. Phys. 102 (1995) 6241.
- [5] H. Kliem, P. Fuhrmann, G. Arlt, IEEE Trans. Electr. Insul. 23 (1988) 919.
- [6] A. Lasia, in: R.E. White, B.E. Conway, J.O.M. Bockris (Eds.), Modern Aspects of Electrochemistry, vol. 32, Plenum Press, New York, 1999, p. 143.
- [7] F. Dion, A. Lasia, J. Electroanal. Chem. 475 (1999) 28.
- [8] J.R. Macdonald, J. Comput. Phys. 157 (2000) 280.
- [9] J.R. Macdonald, Inverse Probl. 16 (2000) 1561.
- [10] J.R. Macdonald, L.D. Potter Jr., Solid State Ionics 23 (1987) 61, The newest WINDOWS version, LEVMW, of the comprehensive LEVM fitting and inversion program may be downloaded at no cost from <http://jrossmacdonald.com>. It includes an extensive manual and executable and full source code. More information about LEVM is provided at this www address.
- [11] E. Tuncer, S.M. Gubanski, IEEE Trans. Dielect. Electr. Insulat. 8 (2001) 310.
- [12] The Monte Carlo DRT program of Ref. [11] is available on request, please contact ET. The routines require Matlab R13 or a newer version.

- [13] J.R. Macdonald, *J. Non-Cryst. Solids* 197 (1996) 83; Erratum: 204 (1996) 309. In addition, in Eq. (A2)  $G_D$  should be  $G_{CD}$ .
- [14] M.E. Orazem, P. Shukla, M.A. Membrino, *Electrochim. Acta* 47 (2002) 2027.
- [15] P. Agarwal, M.E. Orazem, L.H. García-Rubio, *J. Electrochem. Soc.* 139 (1992) 1917; P. Agarwal, O.D. Crisalle, M.E. Orazem, L.H. García-Rubio, *J. Electrochem. Soc.* 142 (1995) 4149; P. Agarwal, M.E. Orazem, L.H. García-Rubio, *J. Electrochem. Soc.* 142 (1995) 4159.
- [16] N. Farag, S. Holten, A. Wagner, H. Kliem, *IEE. Proc. Sci. Meas. Technol.* 150 (2003) 65.
- [17] J.R. Macdonald, in: J.R. Macdonald (Ed.), *Impedance Spectroscopy – Emphasizing Solid Materials and Systems*, John Wiley, New York, NY, 1987, p. 181.
- [18] B.A. Boukamp, J.R. Macdonald, *Solid State Ionics* 74 (1994) 85.
- [19] J.R. Macdonald, *Electrically Based Microstructural Characterization, Symposium Proceedings*, vol. 411, Materials Research Society, Pittsburgh, PA, 1996, pp. 71–83.
- [20] J.R. Macdonald, *Braz. J. Phys.* 29 (1999) 332.
- [21] B.A. Boukamp, *J. Electrochem. Soc.* 142 (1995) 1885.
- [22] E. Tuncer, J.R. Macdonald, *J. Appl. Phys.* 99 (2006) 074106-1.
- [23] J.R. Macdonald, *J. Phys.: Condens. Mat.* 18 (2006) 629, The word “imaginary” on the third line of p. 643 should be replaced by “real”.
- [24] J.R. Macdonald, *J. Phys.: Condens. Mat.* 17 (2005) 4369.
- [25] Z. Stoynov, D. Vladikova, *Differential Impedance Analysis*, Marin Drinov Academic Publishing House, Sofia, Bulgaria, 2005.
- [26] C.T. Moynihan, L.P. Boesch, N.L. Laberge, *Phys. Chem. Glasses* 14 (1973) 122; C.T. Moynihan, *J. Non-Cryst. Solids* 172–174 (1994) 1395.
- [27] J.R. Macdonald, *J. Appl. Phys.* 95 (2004) 1849.